

HOMOGENIZATION OF THE IMPEDANCE PHASE CHARACTERISTICS OF GIANT MAGNETOIMPEDANCE SENSORS

E. Costa Silva^{1,2}, *L. A. P. Gusmão*², *C. R. Hall Barbosa*¹, *E. Costa Monteiro*¹

¹ Postgraduate Program in Metrology, Pontifícia Universidade Católica do Rio de Janeiro (PUC-Rio), Rio de Janeiro, Brazil

² Department of Electrical Engineering, Pontifícia Universidade Católica do Rio de Janeiro (PUC-Rio), Rio de Janeiro, Brazil

Abstract: Over the last decade, Giant Magnetoimpedance (GMI) sensors have been intensively studied as a new possibility for measuring ultra-weak magnetic fields. To achieve that goal, the employment and optimization of gradiometric configurations are a key factor, aiming at reducing the magnetic interference. The homogeneity of the impedance characteristics of GMI sensors is strongly related to the performance of the gradiometers. Then, pursuing the development of better gradiometers, this work aims at presenting a new electronic approach developed by our research group, which leads to the homogenization of the phase characteristics of heterogeneous GMI samples and, consequently, can be used to improve the performance of phase-based GMI magnetometers.

Key-words: Homogenization, Impedance Phase, Giant Magnetoimpedance, Magnetic Sensor.

1. INTRODUCTION

The Giant Magnetoimpedance effect (GMI) began to be intensively studied in the 1990s. It was observed a huge impedance variation when a sample of a ferromagnetic amorphous material, excited by an alternating current, was submitted to an external magnetic field [1-20].

The GMI phenomenon is induced by the application of an alternating current (I) along the length of amorphous ferromagnetic samples, which are submitted to an external magnetic field (H) [1-6]. The impedance of GMI samples changes in function of H , as shown in Fig. 1, and H can be inferred by measuring the difference of potential (V) between the extremities of the GMI sample.

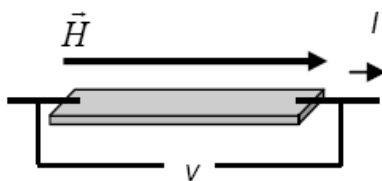


Fig. 1. Typical measurement of the GMI effect: The difference of potential (V) between the extremities of a GMI sample, submitted to an excitation current (I), as a function of the magnetic field (H)

The complex impedance $Z_{sens}(H)$ of the GMI samples can be electrically modeled as a resistor $R_{sens}(H)$ in series with an inductor $L_{sens}(H)$, as defined by (1).

$$Z_{sens}(H) = R_{sens}(H) + j\omega L_{sens}(H), \quad (1)$$

where

$$R_{sens}(H) = |Z_{sens}(H)| \cos \theta_{sens}(H), \text{ and} \quad (2)$$

$$\omega L_{sens}(H) = |Z_{sens}(H)| \sin \theta_{sens}(H). \quad (3)$$

Over the last years, the research group of the Laboratories of Sensors and Instrumentation (LSI) and Biometrology (LaBioMet) of PUC-Rio has worked on the development of transducers based on the GMI effect [7-20]. Recent researches, conducted by the LSI and LaBioMet team allowed observing that phase-based GMI transducers are much more sensitive than the usual magnitude-based GMI transducers [12-20].

The use of phase-based GMI transducers together with the development of a new electronic circuit that allows improving about a hundredfold the impedance phase sensitivity of the GMI sensors [16-17, 20], enabled to envision a new application of the GMI magnetometers, which is the measurement of ultra-weak magnetic fields, such as biomagnetic fields [20-22].

By definition, biomagnetic fields are magnetic fields generated by living organisms or by magnetic markers placed on these organisms. The intensities of the magnetic flux densities of biomagnetic fields are comprised between 1 fT and 1 nT, and their frequencies are in the range of 0 Hz to 1 kHz [20-22].

It is highlighted that nowadays the only magnetometer capable to perform satisfactorily that kind of measurements is the Superconducting Quantum Interference Device (SQUID). Among all the magnetometers (fluxgates, Hall effect, magnetoresistance, etc.), the SQUIDs are the most sensitive. However, SQUID systems have a serious financial drawback, related to its need of cryogenic cooling, characterized by its very high cost of fabrication, installation and operation [5-6, 20-21]. Thus, it limits the broad dissemination of important diagnostic techniques (magnetocardiography, -encephalography, -myography, etc.), based on measurements of biomagnetic fields, due to their dependency on SQUID systems [20-21].

High sensitivity magnetic transducers, capable of measuring ultra-weak magnetic fields, have their resolutions limited by spurious magnetic interference due to diverse sources (vehicles, elevators, Earth's magnetic field, etc.)

which, in a typical laboratory environment, is in the order of 10 nT in the neighborhood of 1 Hz [5, 20-21]. Thus, in principle, no matter how sensitive a transducer is, it cannot detect magnetic fields below the noise/interference level.

To solve that issue, there are two usual approaches: magnetic shielding and gradiometric configurations. In spite of present good results, meaning high attenuation of the magnetic noise and interference, the magnetic shields are very expensive, especially when it's desirable to shield low frequency fields, which significantly affect the measurements of biomagnetic fields, because it requires the use of materials with high magnetic permeability at low frequencies, like μ -metal alloys [20-22].

On the other hand, the other approach, which is much cheaper than the first one and also effective in most applications, consists in the use of gradiometers (spatial filters), relying in the fact that the magnetic field of a dipole decreases with the cube of the distance r . A first-order gradiometric configuration requires two magnetometers with their sensor elements separated by a distance d , making it possible to significantly weaken the contribution of magnetic interference sources located at $r \gg d$ in relation to the contribution of the signal source disposed in $r \ll d$ [20-22].

The performance of the gradiometric configurations is highly dependent of the sensors homogeneity [21-22]. However, it was observed that those experimentally analyzed GMI samples are significantly heterogeneous. Then, this work presents a newly developed method that can be applied to homogenize the impedance phase characteristics of heterogeneous GMI sensors, aiming at the future implementation of GMI gradiometers. It is also proposed and discussed the electronic implementation of the homogenization method.

2. IMPEDANCE CHARACTERIZATION

The GMI sensors analyzed in this work are ribbon-shaped samples of $\text{Co}_{70}\text{Fe}_5\text{Si}_{15}\text{B}_{10}$, produced by the Single-Roller Melt-Spinning technique. These samples show a particular case of the GMI effect, called Longitudinal Magnetoeimpedance (LMI). LMI samples are much more sensitive to the component of the magnetic field parallel to its length.

The sensitivity of the GMI samples is typically affected by some parameters such as amplitude, frequency and DC level of excitation current, dimensions (length, width, thickness) of the GMI samples; biasing magnetic field (generated by an external source to ensure that the sensor operates in its most sensitive range), among others. Therefore, the influence of these parameters under the GMI effect was experimentally investigated in order to ascertain which is the set of parameters that generates the optimum sensitivities [1-4, 20].

Thus, the behavior of the impedance magnitude $|Z_{sens}(H)|$ and phase $\theta_{sens}(H)$ of the ribbon-shaped GMI sensors, as a function of the external magnetic field H , was analyzed under different conditions. It was studied the dependency in relation to the excitation currents of the samples for DC levels between 0 mA and 100 mA, and frequencies between

75 kHz and 30 MHz. Also, it was verified that the amplitude of the AC component of the excitation current does not significantly affect the impedance behavior, so it was held in 15 mA. The influence of the length of the GMI sensors was also investigated. The measurements were performed with four different lengths: 1 cm, 3 cm, 5 cm and 15 cm [12-20].

The analyzed GMI samples were put in the center of a Helmholtz coil, as shown in Fig. 2, in order to be excited by a magnetic field longitudinal to the direction of the current that flows through them. Also, the sample-coil set was positioned in a way to guarantee that the magnitude of the Earth's magnetic field was transversal to the ribbons-shaped GMI samples. Thus, its influence in the measurements has been minimized, because the GMI sensors used are of the LMI type.

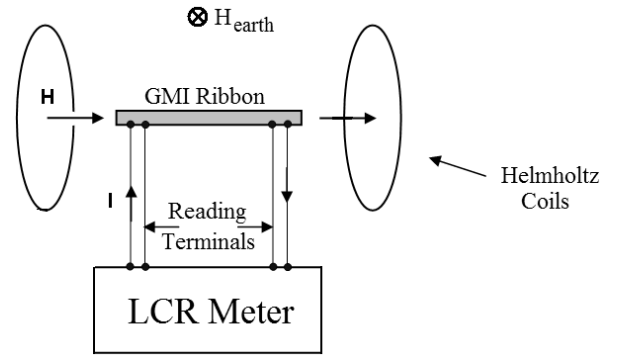


Figure 2. Block diagram of the system used in the experimental characterization of the ribbon-shaped GMI samples.

The magnitude and phase readings were taken by an LCR meter, which was also responsible for both AC and DC excitation of the samples. The variation of the magnetic field generated by the Helmholtz pair was obtained by a DC current source, according to

$$H(Oe) = 2.877 \times I(A). \quad (4)$$

The impedance measurements of the GMI samples, analyzed during the characterization studies, were performed by the precision LCR meter Agilent 4285A. The uncertainty of the impedance phase measurements of the samples U_θ is directly attributed to the impedance phase uncertainty of the LCR meter, which is indicated, in degrees, in its operational manual as

$$U_\theta = \pm \frac{180 \times A_e}{\pi \times 100}, \quad (5)$$

where A_e is defined as

$$A_e(\%) = \pm(A_n + A_c) \times K_t, \quad (6)$$

where A_n is the component of the uncertainty due to the equipment intrinsic characteristics, A_c is the cable length factor and K_t is the temperature factor.

The temperature factor K_t is equal to one in the range of 18°C to 28°C. The measurements were always performed within this temperature range, then it can be admitted that $K_t = 1$. On the other hand, for impedance magnitudes below 5 k Ω , A_c is given by

$$A_c(\%) = \frac{f_m}{15}, \quad (7)$$

where f_m is the frequency, in MHz, used to excite the sample.

Then, knowing that all of the experimental measurements of the impedance magnitudes of the GMI sensors returned values between 10 mΩ and 100 Ω, the parameter A_n is defined as

$$A_n(\%) = N_2\% + \left(\frac{f_m}{30}\right)^2 \times 3\% + \frac{100}{|Z_m|} \left[0.02\% + \left(\frac{f_m}{30}\right) \times 0.1\% \right], \quad (8)$$

where $|Z_m|$ is the absolute value of the measured impedance in ohms and N_2 is a frequency-dependent factor which can be equal to 0.15 – frequencies between 75 kHz and 3 MHz – or to 0.38 – frequencies above 3 MHz.

The standard uncertainty of the magnetic field (u_H) generated by the Helmholtz pair is dependent of the standard uncertainty of the DC current source (ICEL, PS-4000), which is equal to ± 3.25 mA. Then, supposing, by simplicity, that the geometric configuration of the Helmholtz Coils is satisfactorily close to the one considered on the theoretical model and knowing that the relation between the current and the magnetic field generated by the Helmholtz Pair is given by (4), u_H is expressed as

$$u_H(Oe) = \pm 2.877 \times u_I(A) = \pm 9.35 mOe. \quad (9)$$

Thus, the expanded uncertainty U_H , for a confidence level of 95.45%, is

$$U_H = 2 \times u_H = \pm 18.70 mOe. \quad (10)$$

3. PHASE HOMOGENIZATION METHOD

Assuming two heterogeneous GMI sensor elements (A and B), with different behaviors of the impedance phase as a function of the magnetic field (H), this section describes a method that allows the homogenization of the impedance phase behavior of such sensors in a given range of magnetic fields (H_1 to H_2) [20].

The sensor element B should be inserted in an "homogenizer circuit", shown in Fig. 3, in order to generate an equivalent impedance Z_B such as the phase of Z_B in H_1 and H_2 (θ_{1B} and θ_{2B}) becomes equal to the phase of the sensor A in these same points (θ_{1A} and θ_{2A}). Regions should be chosen preferably where there is a linear, or almost linear, dependence between the phase of the GMI sensors and the magnetic field, so that the homogenization procedure can be optimal.

When the sensor B is connected to the "homogenizer circuit" (Fig. 3), it is created an equivalent impedance Z_B , which phase characteristics behaves similarly to the ones of sensor A , within a given magnetic field range. The block reactance shown in Fig. 3 may be replaced by an inductance (L_{adj}) or capacitance (C_{adj}) as required, and the block resistance may represent a positive or negative resistance depending on the case. It is emphasized that the negative resistance can be implemented by a well-known active

electronic configuration called frequency-dependent negative-resistance (FDNR) [23].

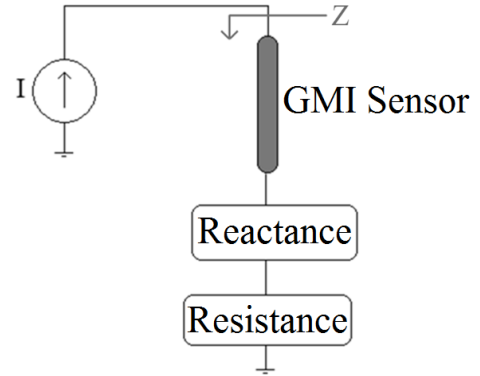


Fig. 3. Block diagram of the "homogenizer circuit"

Setting an arbitrary reactance X_{adj} (inductive or capacitive) and a resistance R_{adj} (positive or negative), which will be placed in series with the sensor B , to homogenize the phase characteristics one should attend [20]

$$\begin{cases} \theta_{1A} = \theta_{1B} \Rightarrow \frac{X_{1A}}{R_{1A}} = \frac{X_{1B} + X_{adj}}{R_{1B} + R_{adj}} \Rightarrow X_{1A}(R_{1B} + R_{adj}) = R_{1A}(X_{1B} + X_{adj}) \\ \theta_{2A} = \theta_{2B} \Rightarrow \frac{X_{2A}}{R_{2A}} = \frac{X_{2B} + X_{adj}}{R_{2B} + R_{adj}} \Rightarrow X_{2A}(R_{2B} + R_{adj}) = R_{2A}(X_{2B} + X_{adj}) \end{cases} \quad (11)$$

By solving the system of equations presented in (11), it is highlighted that X_{adj} may return either a positive value (meaning that X_{adj} is an inductance L_{adj}) or a negative value (meaning that X_{adj} is a capacitance C_{adj}), leading to

$$L_{adj} = \frac{X_{adj}}{\omega} \quad \text{or} \quad C_{adj} = -\frac{1}{\omega X_{adj}}. \quad (12)$$

4. RESULTS AND DISCUSSION

Fig. 4 shows the phase characteristics of two GMI ribbon-shaped sensor elements (A and B), both of them 3 cm long and submitted to the same excitation current - DC level of 80 mA, 15 mA of amplitude and 100 kHz of frequency. All of the impedance phase values shown in this section have their respective measurement uncertainties U_{θ} , obtained by applying (5), equal or smaller than $\pm 1^\circ$.

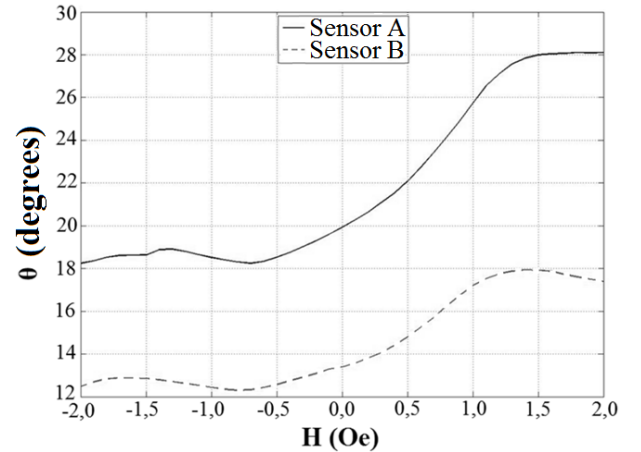


Fig. 4. Impedance phase characteristics, of heterogeneous GMI samples (A and B), as a function of the external magnetic field.

In turn, Figs. 5 and 6 represent, respectively, the dependence of the resistance (R_{sens}) and inductance (L_{sens}), as a function of magnetic field (H), for the same GMI sensors A and B whose phase characteristics are presented in Fig. 4.

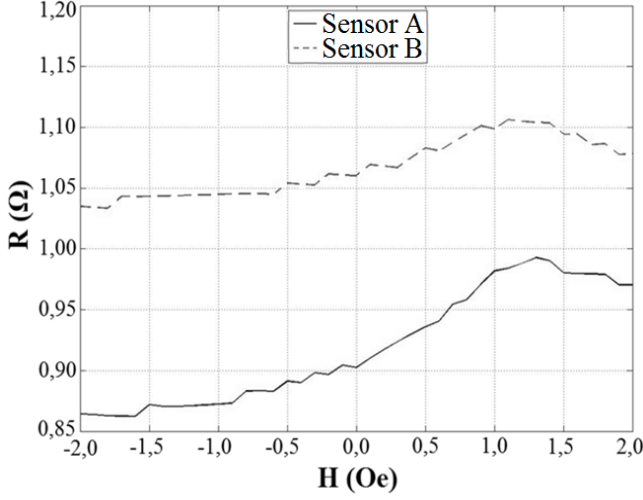


Fig. 5. Characteristics of the resistive component of the impedance, of heterogeneous GMI samples (A and B), as a function of the external magnetic field

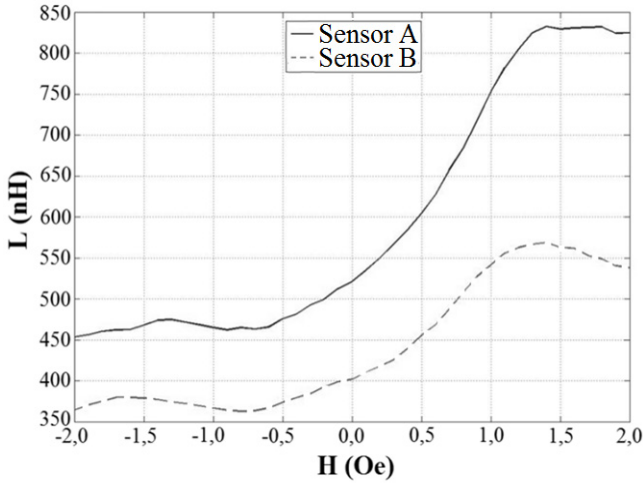


Fig. 6. Characteristics of the reactive (inductive) component of the impedance, of heterogeneous GMI samples (A and B), as a function of the external magnetic field

Sensors A and B are clearly heterogeneous, then it is aimed to make the phase behavior of sensor B similar to the phase behavior of sensor A , in the region between $H_1 = 0.3$ Oe and $H_2 = 1.0$ Oe ($1 \text{ Oe} = 10^3/4\pi \text{ A/m}$). Thus, the homogenization can be accomplished by applying the experimental data of R_{sens} and L_{sens} , obtained from sensors A and B , on the system of equations defined in (11). The following parameters of interest were used: $R_{1A} = 0.9237 \Omega$, $L_{1A} = 566.7 \text{ nH}$, $R_{2A} = 0.9819 \Omega$, $L_{2A} = 753.1 \text{ nH}$, $R_{1B} = 1.0670 \Omega$, $L_{1B} = 425.6 \text{ nH}$, $R_{2B} = 1.0990 \Omega$, $L_{2B} = 541.2 \text{ nH}$. With these parameters it is possible to solve the system given by (11), obtaining

$$\begin{cases} R_{adj} = -0.4737\Omega \\ X_{adj} = -0.0387 \Rightarrow C_{adj} = -\frac{1}{\omega X_{adj}} = 41.12\mu\text{F} \end{cases} \quad (13)$$

Fig. 7 compares the phase characteristics of sensor A with the ones of the equivalent impedance Z_B , generated by the insertion of sensor B in the electronic circuit of Fig. 3, and using the reactance and resistance values given by (13).

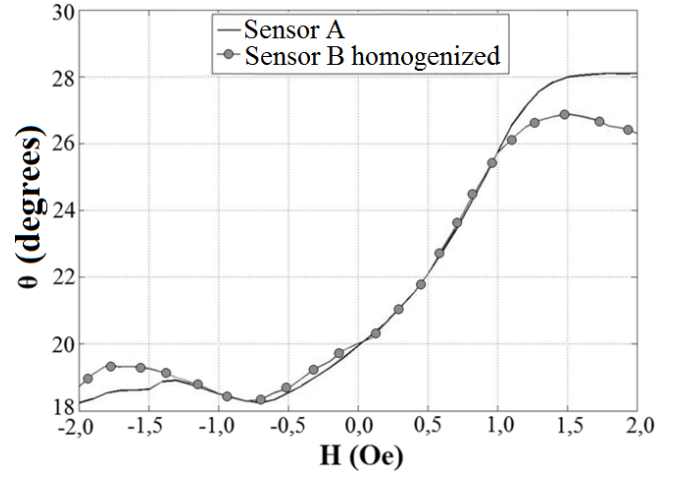


Fig. 7. Comparison between the impedance phase characteristics of sensor A and sensor B, with sensor B connected to the "homogenizer circuit"

On the other hand, Fig. 8 shows the point-to-point error, in degrees, between the phase curves, shown in Fig. 7, as a function of the magnetic field. The analysis in Fig. 8 is presented for the region of magnetic fields where the homogenization was applied (0.3 Oe to 1.0 Oe). By observing Figs. 7 and 8 it is possible to note that the proposed procedure of homogenization was fairly successful, generating satisfactorily alike phase characteristics.

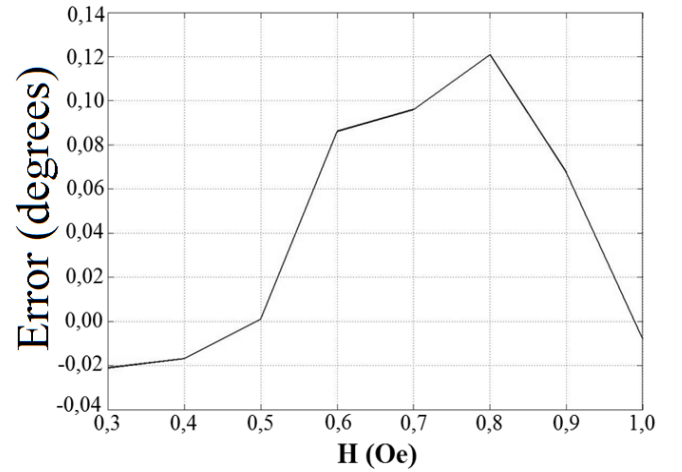


Fig. 8. Error in the homogenized region (0.3 Oe to 1.0 Oe) between the phase curves of sensor A and sensor B, when the last one is connected to the "homogenizer circuit"

Comparisons between the resistive components of sensors A , B , and B connected to the "homogenizer circuit" and between their inductive components are shown, respectively, in Figs. 9 and 10. At a first thought, it could be expected that by inserting the sensor B in the "homogenizer circuit" would lead to having their resistive and inductive components similar to those presented by sensor A . However, by observing Figs. 9 and 10, it is noticed that this did not happen.

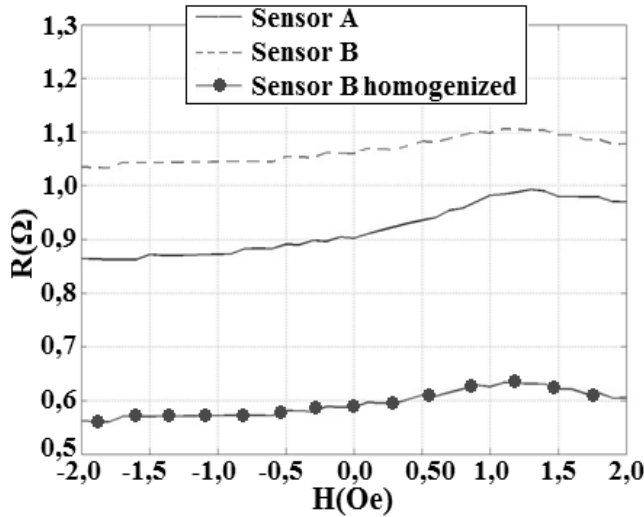


Fig. 9. Comparison between the resistive components of the GMI sensors: A, B and B connected to the “homogenizer circuit”

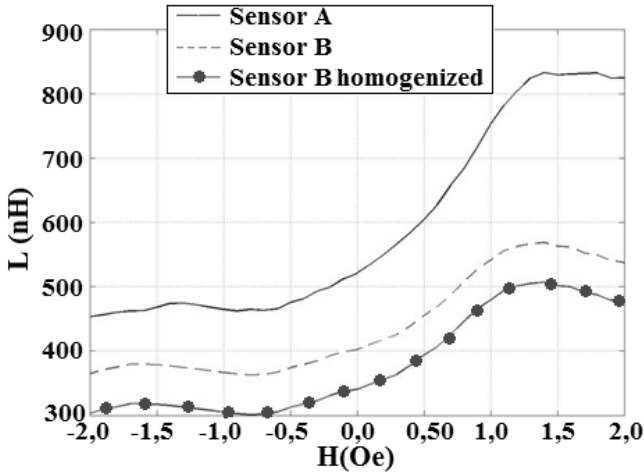


Fig. 10. Comparison between the inductive components of the GMI sensors: A, B and B connected to the “homogenizer circuit”

Actually, that did not happen because the aim of the homogenization process is putting as close as possible (homogenize) the phase characteristics of heterogeneous sensors, in a defined magnetic field region, which does not necessarily implies in also homogenizing the characteristics of the resistive and reactive components of the sensors.

It is highlighted that, in the region of interest (0.3 Oe to 1.0 Oe), sensor *A* has a higher sensitivity than sensor *B*. The applied method aimed at making the phase behavior of sensor *B* similar to the one presented by sensor *A*, so it was concluded that one should use a capacitor and a negative resistance in series with sensor *B*. However, if the purpose was the opposite, i.e. making the phase behavior of sensor *A* similar to the one presented by *B*, it should be used a positive resistance and an inductor in series with sensor *A* [20]. More specifically, in that case, solving (11) leads to

$$\begin{cases} R_{adj} = 0.762\Omega \\ X_{adj} = 0.06641 \Rightarrow L_{adj} = \frac{X_{adj}}{w} = 105.7nH \end{cases} \quad (14)$$

5. CONCLUSION

This paper presented a new method capable of homogenizing the impedance phase characteristics of heterogeneous GMI sensors. It was also described an electronic circuit, called “homogenizer circuit”, which can be used on the implementation of the proposed method.

The results obtained demonstrate the effectiveness of the developed homogenization method, as shown in Figs. 7 and 8, allowing that GMI sensors with different phase behaviors, after inserted in the developed “homogenizer circuit”, evolve to almost homogeneous phase behaviors.

In a future work, a gradiometric configuration will be implemented using the developed “homogenizer circuit”, aiming at improving the quality of the gradiometric readings and, consequently, enhancing the performance of phase-based GMI magnetic transducers.

ACKNOWLEDGEMENTS

We thank the Brazilian funding agencies CNPq and FINEP, for their financial support, and Prof. Fernando Luis de Araújo Machado (Department of Physics / UFPE) for the GMI samples provided.

REFERENCES

- [1] L. A. P. Gonçalves, J. M. Soares, F. L. A. Machado, W. M. de Azevedo, “GMI effect in the low magnetostrictive CoFeSiB alloys”, *Physica B*, v. 384, pp. 152-154, 2006.
- [2] V. Knobel, K. R. Pirota, “Giant magnetoimpedance concepts and recent progress,” *J. Magn. Magn. Mater.*, v. 242, pp. 33–40, 2002.
- [3] H. Hauser, L. Kraus and P. Ripka, “Giant magnetoimpedance sensors,” *IEEE Instrum. Meas. Mag.*, vol. 4, no. 2, pp. 28–32, 2001.
- [4] M. H. Phan and H. X. Peng, “Giant magnetoimpedance materials: Fundamentals and applications”, *Prog. Mat. Sci.*, vol. 53, pp. 323-420, 2008.
- [5] A. E. Mahdi, L. Panina, D. Mapps, “Some new horizons in magnetic sensing: high-*T_c* SQUIDS, GMR and GMI materials”, *Sensors and Actuators A*, v. 105, pp. 271–285, 2003.
- [6] J. Lenz, A. S. Edelstein, “Magnetic sensors and their applications”, *IEEE Sensors Journal*, vol. 6, n. 3, pp. 631-649, 2006.
- [7] C. R. Hall Barbosa, E. Costa Monteiro, F. M. P. Cavalcanti, “Localization of Magnetic Foreign Bodies in Humans using Magnetic Field Sensors”, *Proceedings of XVII IMEKO World Congress - Metrology in the 3rd Millennium*. Zagreb: HMD - Croatian Metrology Society, p.1510–1513, 2003.
- [8] F. Pompéia, L. A. P. Gusmão, C. H. Barbosa, E. Costa Monteiro, L. A. P. Gonsalves, F. L. A. Machado, “Development of a Low Intensity Magnetic Field Transducer for Biomedical Application based on the

- Giant Magnetoimpedance Effect”, *Proceedings of the Joint International IMEKO TC1+ TC7 Symposium*, 2005.
- [9] F. Pompéia, L. A. P. Gusmão, C. R. Hall Barbosa, E. Costa Monteiro, L. A. P. Gonçalves, F. L. A. Machado, “Characterization of a Magnetic Field Transducer based on the GMI Effect”, *Proceedings of the XVIII IMEKO World Congress - Metrology for a Sustainable Development*, 2006.
- [10] D. Ramos Louzada, E. Costa Monteiro, L. A. P. Gusmão, C. Hall Barbosa, “Medição não-invasiva de ondas de pulso arterial utilizando transdutor de pressão MIG”, *Proceedings of the IV Latin American Congress on Biomedical Engineering*, C. Mueller-Karger, S. Wong, A. La Cruz (Eds.): CLAIB 2007, IFMBE Proceedings 18, pp. 436–439, 2007.
- [11] F. M. P. Cavalcanti, L. A. P. Gusmão, C. R. H. Barbosa, E. Costa Monteiro, L. A. P. Gonçalves, F. L. A. Machado, “Ring shaped magnetic field transducer based on the GMI effect”, *Measurement Science & Technology*, v. 19, pp. 1-10, 2008.
- [12] E. Costa Silva, L. A. P. Gusmão, C. Hall Barbosa, E. C. Monteiro, “Magnetic field transducers based on the phase characteristics of GMI sensors and aimed to Biomedical Applications”, *Proceedings of the 13th ICBME*, Singapore, v. 23, pp. 652-656, 2009.
- [13] E. Costa Silva, L. A. P. Gusmão, C. R. Hall Barbosa, E. Costa Monteiro, “Transdutor de pressão, baseado nas características de fase do efeito GMI, para detecção de ondas de pulso arterial”, *Anais do VIII SEMETRO*, João Pessoa, 2009.
- [14] E. Costa Silva, L. A. P. Gusmão, C. R. H. Barbosa, E. Costa Monteiro, “Transdutor de pressão, baseado nas características de fase do efeito GMI, destinado a aplicações biomédicas”, *Controle & Automação*, v. 21, n. 6, pp. 598-608, 2010.
- [15] E. Costa Silva, L. A. P. Gusmão, C. R. H. Barbosa, E. Costa Monteiro, F. L. A. Machado, “High sensitivity giant magnetoimpedance (GMI) magnetic transducer: magnitude versus phase sensing”, *Measurement Science & Technology*, v. 22, pp. 1-9, 2011.
- [16] E. Costa Silva, L. A. P. Gusmão, C. R. H. Barbosa, E. Costa Monteiro, “Amplificação da sensibilidade de fase de sensores GMI para medição de campos biomagnéticos”, *Anais do XXII Congresso Brasileiro de Engenharia Biomédica*, Tiradentes, 2010.
- [17] E. Costa Silva, L. A. P. Gusmão, C. R. H. Barbosa, E. Costa Monteiro, “Progress Toward a Hundredfold Enhancement in the Impedance Phase Sensitivity of GMI Magnetic Sensors aiming at Biomagnetic Measurements”, *Proceedings of the V Latin American Congress of Biomedical Engineering*, CLAIB 2011, Havana, 2011.
- [18] PUC-Rio. Pontifícia Universidade Católica do Rio de Janeiro. E. Costa Silva, L. A. P. Gusmão, C. Hall Barbosa, E. Costa Monteiro, F. L. A. Machado, F. Pompéia, D. R. Louzada, *Patent*, **BR PI 0902770-0**, February 17, 2009.
- [19] PUC-Rio. Pontifícia Universidade Católica do Rio de Janeiro. E. Costa Silva, L. A. P. Gusmão, C. Hall Barbosa, E. Costa Monteiro, F. L. A. Machado, F. Pompéia, D. R. Louzada, *Patent*, **WO/2010/094096**, February 12, 2010.
- [20] E. Costa Silva, “Development of a transducer based on the phase of the giant magnetoimpedance for the measurement of biomagnetic Fields”, *Master Thesis*, Postgraduate Program in Metrology, Pontifícia Universidade Católica do Rio de Janeiro, 2010.
- [21] W. Andrä, H. Nowak, *Magnetism in Medicine: A Handbook*, 2 ed. Weinheim: WILEY-VCH Verlag GmbH & Co. KGaA. 2007.
- [22] J. Clarke, A. I. Braginski, *The SQUID Handbook*, 2. ed., Weinheim: WILEY-VCH Verlag GmbH. 2006.
- [23] L. T. Bruton, *RC-Active Circuits: Theory and Design*, London: Prentice-Hall International. 1980.